REAL-TIME BAYESIAN GSM BUZZ REMOVAL

Han Lin, Simon Godsill

Signal Processing Group, Department of Engineering
University of Cambridge
Trumpington Street, Cambridge CB2 1PZ, UK
{HL309|SJG30}@cam.ac.uk

ABSTRACT

In this paper we propose an iterative audio restoration algorithm based on an autoregressive (AR) model with modeling of the noise pulse template to detect and restore Cell-phone electromagnetic interference (EMI) patterns known as "GSM buzz". The algorithm is purely software based and does not require the aid of any hardware providing side information. The only assumption is that individual pulses are similar to scaled versions of the known template. With this assumption, the algorithm can fully detect and restore noisy interference signals in real time with almost no audible artifacts and improve the signal to noise ratio by as much as 50dB.

1. INTRODUCTION

TDMA, CDMA and GSM are the three most common digital signals used by cellular service providers. These wireless transmission protocols send out strong electromagnetic pulses as control or data signals during the registration process as well as during receiving, transmitting, and hand-over procedures. Once transmitted, interference pulses are received by audio amplifiers and line-in circuits, which generates audible sound distortion in the form of "GSM buzz" (217 Hz for full rate and 108 Hz for half rate) [1] [2].

Although audio products such as car stereos, telephones, recorders, portable audio players, medical devices [3], and hearing aids [4] all suffer from this kind of interference, such interference is often ignored. However, as the popularity of cellular phones grows, the problem can no longer be overlooked, especially for high-end consumer audio products and hearing aids that place emphasis on the clarity of the sound.

Reducing Cell-phone transmission power, changing the transmission protocol, equipping a telecoil [5], as well as shielding the audio circuit can alleviate the problem. However, these solutions cannot be implemented without changing the existing hardware designs, which can often be very difficult and expensive. In addition, building an interference-free audio circuit that is immune from the noises caused by electromagnetic pulses transmitted using various protocols (GSM, TDMA, and CDMA) is nearly impossible. Further, interference can happen in any phase of the audio transmission path, and once the audio waveform is interfered with, there is no existing solution to filter out the noise without distorting the original audio.

For many industry applications, internal subtractive noise cancellation where a regenerated noise pulse is fed back to the circuit and subtracted from the signal provides an effective solution [6] [7]. However, the design is only practical when the regenerated noise pulse is exact. Generally this is achieved with the aid of a hardware detector and a synchronized hardware clock generator. Other solutions such as notch filter based restoration [2] typically require frequency domain operation, produce a metallic sound, and most importantly, rely on the fact that individual pulses arrive at exact and regular intervals (217 Hz for full rate) without any delays, which is rare when a mobile phone is trying to connect with the base stations during call initialization and hand-over [8].

Many efficient real-time audio restoration algorithms are based on autoregressive (AR) model, where a stationary random audio signal is modeled as the output of an order P all-pole filter excited by white noise. In the AR model, the output of a linear time invariant filter is restricted to a weighted sum of past output values and a white noise input $e_{AR}(n)$ [9].

$$s(n) = \sum_{i=1}^{P} a(i)s(n-i) + e_{AR}(n)$$

A statistical signal processing approach based on the AR model with prior knowledge of noise pulse template is applied to restore Cell-phone interfered audio files. The approach intends to detect and remove Cell-phone interfered noise pulses before the audio data is played back on the speaker/headphone, or after the audio files are recorded. The restoration process is extremely effective and it is performed at the last stage of the audio circuit.

2. ANALYSIS OF NOISE PULSE AND THE RESTORATION MODEL

When Cell-phone induced electromagnetic interference pulses, in the form of a square wave, interfere with an audio signal, the pulses are superimposed onto the original waveform. A typical corrupted, Cell-phone interfered, audio signal $x(n)$ appears as in Fig. 1. We can see in Fig. 2 a typical noise pulse $g(n)$ consists of two main parts: a *central pulse* and a *decaying tail*. The *central pulse* is caused by the electromagnetic (EM) excitation and the *decaying tail* is due to the capacitance associated with the audio circuit. Therefore, we consider an idealized model of the corrupted signal. This model is used in section 3 to devise an detector. In section 4, an iterative restoration procedure loosely based on the idealized model is provided.

$$x(n) = bg(n-m) + s(n) + e(n) \tag{1}$$

Where:

- $x(n)$ is the observed corrupted, Cell-phone interfered signal,
- $g(n)$ is the known interference pattern template of Cell-phone interference noise pulse,

- b is a constant scaling factor to compensate for the amplitude difference between noise and template,
- $e(n)$ is a white output noise,
- $s(n)$ is the original signal without interference.

We can see that if the exact start location m of the Cell-phone interference template $g(n)$ is known, and if we can also determine the scaling factor b, we can then restore the original signal $s(n)$.

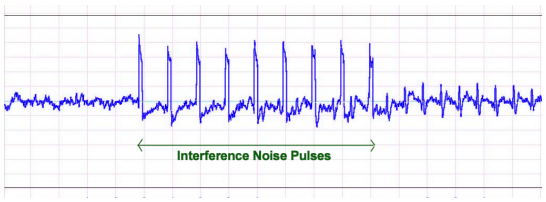

Figure 1: $x(n)$ - *A typical section of cell-phone interfered audio.*

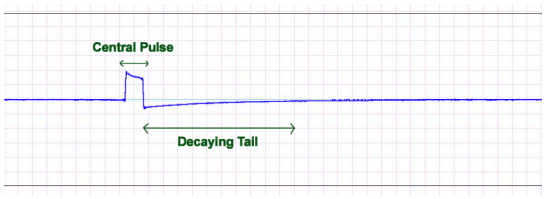

Figure 2: $g(n)$ - *A typical cell-phone interference noise pulse.*

3. DETECTION OF NOISE PULSES

Numerous detection methods can be used to determine the exact location of the noise pulses, for example:

1. Hardware electromagnetic wave detector,
2. Threshold detection from signal,
3. Threshold detection from signal slope,
4. Cross correlation/matched filter detector,
5. Bayesian step detector [10] (chapter 5),
6. Autoregressive (AR) detector [9] (chapter 5),
7. The *Bayesian template detector* (see section 3.1)

For real-time applications, a hardware electromagnetic wave detector can be an effective solution. For software implementations, threshold detection from signal amplitude can be a simple and efficient method. Threshold detection from signal slope can also be very effective.

3.1. The Bayesian Template Detector

To increase accuracy, the exact location of the *central pulse* can be calculated with a *Bayesian template detector* model. The model helps to predict the probability associated with each possible pulse location. We can then detect the location of the noise pulse by determining the value of m which produces the maximum probability, where m is the start of the noise pulse. Here we create the *Bayesian template detector* model by simplifying Eq. (1) with $e(n) = 0$:

$$x(n) = bg(n-m) + s(n) \tag{2}$$

$s(n)$ is assumed to be autoregressive:

$$s(n) = \sum_{i=1}^{P} a(i)s(n-i) + e_{AR}(n)$$

And we can write:

$$\mathbf{e}_{AR} = \mathbf{A}\mathbf{s}$$

$\mathbf{A}$ is a $((N-P)\times N)$ matrix containing autoregressive coefficients (see [9] for detailed description of $\mathbf{A}$). We can then rewrite Eq. (2) as:

$$\mathbf{e}_{AR} = \mathbf{A}(\mathbf{x} - b\mathbf{g})$$

Where $\mathbf{g} = [g(-m)\ \ g(-m+1)\cdots g(N-1-m)]^{\mathbf{T}}$. We assume $\mathbf{e}_{AR}$ is a zero mean independent Gaussian vector with variances σ_1^2 , i.e. $P(e_{AR}(n)) = N(0, \sigma_1^2)$. b is a Gaussian variable with mean b' and variance $k\ \sigma_1^2$, i.e. $P(b) = N(b', k\sigma_1^2)$. k is generally a large constant. We now obtain the equation for $P(\mathbf{x}|m, b)$:

$$P(\mathbf{x}|m, b, \sigma_1) \propto P_{e_{AR}}(\mathbf{A}(\mathbf{x}-b\mathbf{g})) \propto (2\pi\sigma_1^2)^{-\frac{N}{2}} \cdot e^{-\frac{1}{2\sigma_1^2}(\mathbf{e}_{AR}^T \mathbf{e}_{AR})}$$

We wish to integrate out parameters b and σ_1 in the detector to obtain an equation in just variable m. We define $\mathbf{u} = \mathbf{A}\mathbf{x}$ and $\mathbf{v} = \mathbf{A}\mathbf{g}$. We can then define the probability model for the *Bayesian template detector*:

$$P(m|\mathbf{x}, \mathbf{g}) = \int p(\mathbf{x}|m, b, \sigma_1)p(m)p(b)p(\sigma_1)dbd\sigma_1 \tag{3}$$

Assigning uniform prior to $p(m)$ and Jeffrey's prior $\frac{1}{\sigma_1}$ for $p(\sigma_1)$ in Eq. (3), σ_1 can be integrated out using the gamma integral [11], b can be obtained using properties of Gaussian integrals, and after rearranging, we have the general solution for the *Bayesian template detector*:

$$P(m|\mathbf{x}, \mathbf{g}) \propto \frac{1}{k\sqrt{\mathbf{v}^T\mathbf{v} + \frac{1}{k^2}}} \cdot \left[\frac{(\mathbf{u}^T\mathbf{v} + \frac{1}{k^2}b')^2}{(\mathbf{v}^T\mathbf{v} + \frac{1}{k^2})} - (\mathbf{u}^T\mathbf{u} + \frac{1}{k^2}b')\right]^{-(\frac{N-P-1}{2})}$$

Empirically, k can be set to a large value and b' is generally zero due to the fact that b can be both positive or negative and no particular value is favored *a priori*.

3.2. Other Detection Methods

Other suitable detection methods include cross-correlation detector, Bayesian step detector, and autoregressive (AR) detector, which are summarized below: A cross-correlation detector correlates the observed signal $x(n)$ with the Cell-phone interference template $g(n)$. A Bayesian step detector was described in detail in [10]. For example, if we assume the observed signal $x(i)$ has mean μ_1 before change point m and mean μ_2 after point m,

$$x(i) = \begin{cases} \mu_1 + \varepsilon(i) & \text{if } i < m \\ \mu_2 + \varepsilon(i) & \text{otherwise} \end{cases}$$

The solution of the simplified Bayesian step detector is then:

$$p(m|\mathbf{x}) \propto \frac{[\mathbf{x^T x} - \mathbf{x^T L}(\mathbf{L^T L})^{-1}\mathbf{L^T x}]^{-\frac{(N-M)}{2}}}{\sqrt{\det(\mathbf{L^T L})}}$$

where $\mathbf{L}$ has two columns. The first column contains m rows of 1s followed by $N-m$ rows of 0s and the second column consists of m rows of 0s followed by $N-m$ rows of 1s. The autoregressive (AR) detector was described in detail in [9] with the following steps:

1. Calculate prediction error $\epsilon_n = x_n - \sum_{i=1}^{P} a_i x_{n-i}$, where x_n is the observed data, ϵ_n is a white noise input, a_i is the AR coefficient, and P is the AR model order,
2. If $|\epsilon_m| > r\sigma_e$, where r is around 3 and σ_e is the standard deviation of the white noise input, m is a possible location for the start of the *central pulse*.

3.3. Comparison of the Different Detectors

For the *Bayesian template detector* and the Bayesian step detector, we plot the probability of noise pulse location according to different possible locations m. For the AR detector, the errors ϵ_n are plotted. On the other hand, for the cross-correlation detector, the aligned cross-correlation results are plotted. For the plots described above, if the values are above a certain threshold, they show indications of possible noise pulse locations. The maximum value indicates the most probable noise pulse location. We can see in Fig. 3 that the Bayesian template detector and the cross correlation detector perform best in finding the noise pulse locations. On the other hand, Fig. 10 shows the AR detector and the simple Bayesian step detector will try to detect both the rising and the falling edges of the noise pulse. This sometimes causes confusion and sacrifices the performance of the detector. Empirical results show that the Bayesian template detector is most precise and robust for most scenarios owing to the fact that location m tends to show up as a very sharp peak. In addition, the Bayesian template detector can be very flexible in the sense that by setting $g(n-m)$ to zero, we can also determine the probability of the "no interference" condition.

4. REMOVAL OF CELL-PHONE INTERFERED NOISE PULSES WITH THE AR TEMPLATE INTERPOLATOR

Once the exact locations of the Cell-phone interference template $g(n)$ are known, say m', we can attempt to remove the noise pulses. We propose a sequential iterative *AR template interpolator* that restores the noise pulses one by one. We first divide the observed corrupted signal $x(n)$ into overlapping frames. The frames should be small enough so that only one pulse can be present at a time. Then for each frame, find the *central pulse* location with any of the detection methods mentioned above. We then restore the *central pulse* location with the AR model and obtain the initial estimate $s^0(n)$ of the clean original signal $s(n)$. Subsequently, we subtract $s^0(n)$ from the observed corrupted signal $x(n)$ to determine the estimated interference signal $r^0(n)$. Further, we fit the interference template $g(n-m')$ to this estimated interference signal $r^0(n)$ to determine the first scaling factor b^1. Then we subtract the scaled template $b^1 g(n-m')$ from the observed corrupted signal $x(n)$ and interpolate over the *central pulse* location again to re-estimate the original signal. The algorithm can then be iterated

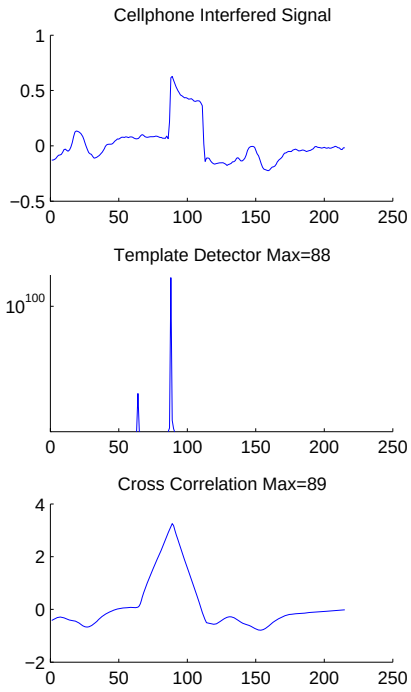

Figure 3: *Detection results of Log of Bayesian template detector and cross correlation detector.*

by using this "re-estimated" signal to determine the scaling factor, which later determines another estimate of the original signal and so on. The exact steps of the *AR template interpolator* are described below:

1. **LSAR** interpolation over the central region of the noise pulse, according to the formula:

$$\mathbf{s}^i = \mathbf{LSAR}(x(n) - b^i g(n-m')) \qquad (4)$$

where i starts from 0 and $b^0 = 0$. Therefore **LSAR** initially restores the *central pulse* (see Fig. 2) location using the AR model [9] ($x(n) = \sum_{i=1}^{P} a(i)x(n-i) + e_{AR}(n)$) with a low order (typical $P = 20$). We know from [9], for example, the solution for the LSAR interpolator is

$$\mathbf{s}^0 = -(\mathbf{A}_{(\mathbf{i})}^{\mathbf{T}}\mathbf{A}_{(\mathbf{i})})^{-\mathbf{1}}\mathbf{A}_{(\mathbf{i})}^{\mathbf{T}}\mathbf{A}_{-(\mathbf{i})}\mathbf{x}_{-(\mathbf{i})}.$$

See [9] for detailed descriptions of $\mathbf{A}$, $\mathbf{A}_{(\mathbf{i})}$, and $\mathbf{A}_{-(\mathbf{i})}$. $\mathbf{x}_{-(\mathbf{i})}$denotes known/ uncorrupted samples of the observed signal $\mathbf{x}$. This is the initial estimate of the original signal $s^0(n)$ (see Fig. 4). Note that $s^0(n)$ is the result of an LSAR interpolator with no prior knowledge of the noise template $g(n)$.

2. We introduce a new variable $r^i(n)$ which represents the estimated interference signal:

$$r^i(n) \equiv x(n) - s^i(n)$$

3. Calculate the next estimate of the scaling factor b^{i+1}; one simple way to do this is to solve the following equation by

minimizing $e(n)$ within the *central pulse* location (see Fig. 6):

$$r^i(n) = b^{i+1}g(n-m') + e(n) \quad (5)$$

4. Finally we set $i = i + 1$ and iterate from 1.

We can see that $s^1(n) = \mathbf{LSAR}(x(n) - b^1 g(n-m'))$ where the fitted interference pulse $b^1 g(n-m)$ has $n \in$ *central pulse* and *decaying tail*. The first estimate of the original signal $s^1(n)$ is shown in Fig. 5. We can also see from Fig. 4, 5 that the first estimate of the original signal $s^1(n)$ is closer to the actual values of the original signal $s(n)$ than the initial estimate of the original signal $s^0(n)$.

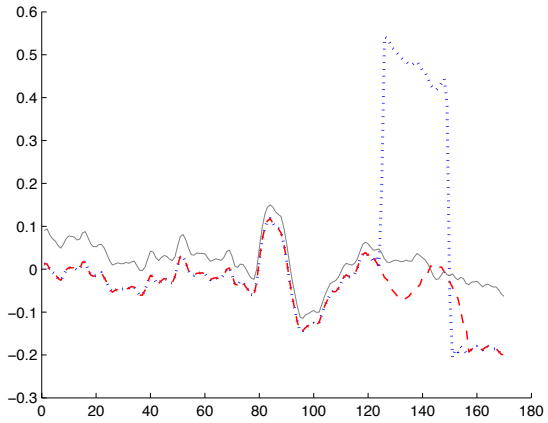

Figure 4: *Example implementation of Eq. (4) : Observed corrupted signal $x(n)$ (Dotted), Original signal $s(n)$ (Gray), Initial estimate of the original signal $s^0(n)$ (Dashed).*

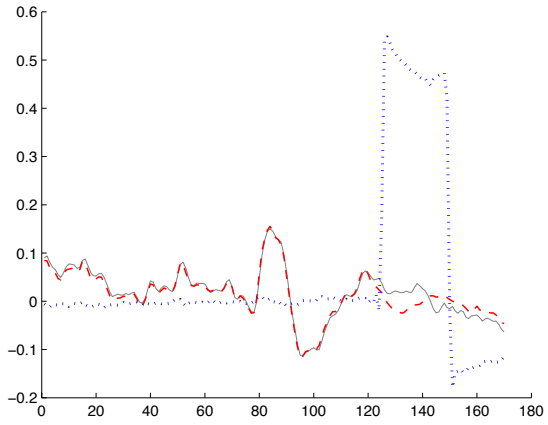

Figure 5: *Example implementation of* Eq. (4) *: Predicted interference pulse $b^1 g(n-m')$ (Dotted), Original signal $s(n)$ (Gray), First estimate of the original signal $s^1(n)$ (Dashed).*

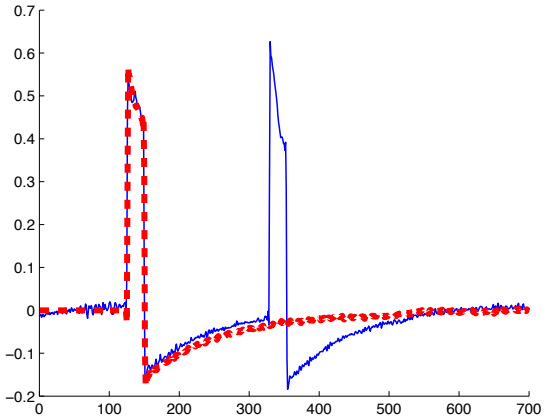

Figure 6: *Eq. (6) : Estimated interference signal $r^0(n)$ (Blue), Fitted interference pulse $b^1 g(n)$ (Dashed).*

5. CONCLUSIONS AND RESULTS

Empirical results show the proposed Bayesian template detector is very effective in detecting the interference pulses. Once the pulses are properly detected, the proposed *AR template interpolator* can typically improve the signal to noise ratio (SNR) of the observed corrupted signal by more than 50dB (Table 1). The *AR template interpolator* outperforms the general LSAR interpolator by as much as a 25dB improvement in SNR. Subjective listening tests show that the *AR template interpolator* restored signal displays no audible artifact when compared to the original signal. The general LSAR interpolator does not take into account the *decaying tail*. We can see from Fig. 7, 11 that the general LSAR interpolator restored signal has a "dip" at the end of the noise pulses. This contributes to the audible artifacts associated with the general LSAR interpolator. Audio samples of the results of the *AR template interpolator* can be found at:

http://www-sigproc.eng.cam.ac.uk/~hl309

- Recorded on a full rate GSM interfered stereo			
- All units in (dB)	**Type of audio signal**		
Restoration techniques	Jazz	Pop	Speech
Noisy signal $x(n)$	-17.0	-25.5	-22.8
LSAR interpolator	19.0	-3.4	1.6
AR template (1st iter)	37.8	18.3	22.8
AR template (5th iter)	38.5	19.5	23.5

Table 1: *SNR performance of different interpolators.*

For time-critical applications, we can use a threshold detector or hardware electromagnetic detectors and restore the corrupted signal with only one iteration of the *AR template interpolator* and no overlap between frames. Then the dominating factor for the complexity is the matrix inversion step in the *AR template interpolator*. The performance of the *AR template interpolator* is of the same order as the general LSAR interpolator. If we use the Levinson-Durbin recursion [12] for the matrix inversion steps we arrive at a computational complexity of $O(L^2)$. For example, if we need to restore a CD quality (44 kHz sampling rate), full rate

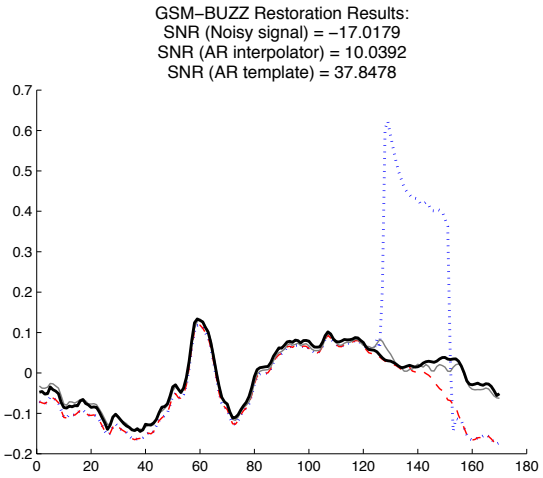

Figure 7: *Example of GSM buzz restoration of a corrupted trumpet sequence (Jazz) :* $x(n)$*(Dotted),* $s(n)$ *(Gray),* $s^0(n)$ *(Dashed),* $s^1(n)$ *(Black).*

217 Hz GSM buzz interfered audio file, L is around 25 to 75 samples (25 samples are the length of the *central pulse*). We can see that with such computational complexity, the algorithm can be efficiently implemented on most microprocessors to run on real-time.

6. FUTURE WORK

The model for removal of Cell-phone interfered noise pulses can be elaborated if we also want to recover the information from the corrupted signal $x(n)$ in the *central pulse* Fig. 2. By observing the patterns of the *central pulse* and the *decaying tail* of the Cell-phone interference noise pulse, we introduce a new variable $y(n)$ to represent the interference noise. We can see from Fig. 8, $y(n)$ can be modeled as two exponential decays. We propose the *Exponential Decay Model* for the observed corrupted signal $x(n)$. We can then estimate the parameters jointly with Bayesian motived techniques such as *Expectation Maximization* or *Gibbs Sampler* [9][10].

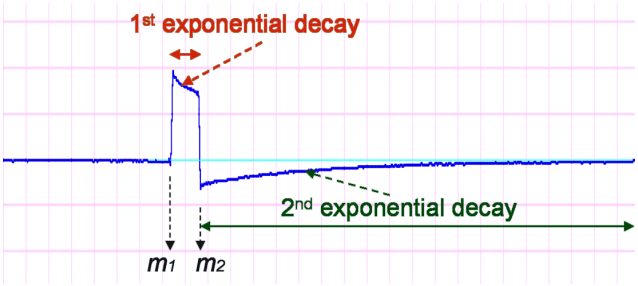

Figure 8: *Example of modeling the noise pulse* $y(n)$ *as 2 exponential decays.*

The Cell-phone interfered noise pulse restoration can be further expanded to the Multi-Channel case, where N channels of audio samples are observed. We can model the noise pulse of one channel as a scaled version of the noise pulse of the other channel (see Fig. 9). We can now extend the AR template interpolator to Multi-Channel [13]. In addition, we can iterate over all the available channels with the *Exponential Decay Model* mentioned earlier.

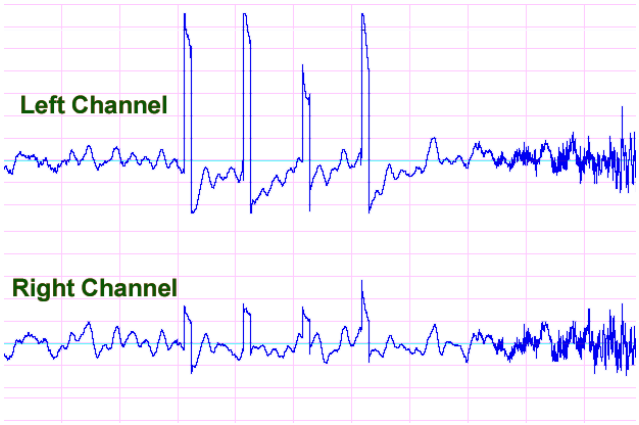

Figure 9: *Example of a cell-phone interfered audio signal where noise pulse of the left channel can be modeled as a scaled version of the noise pulse of the right channel.*

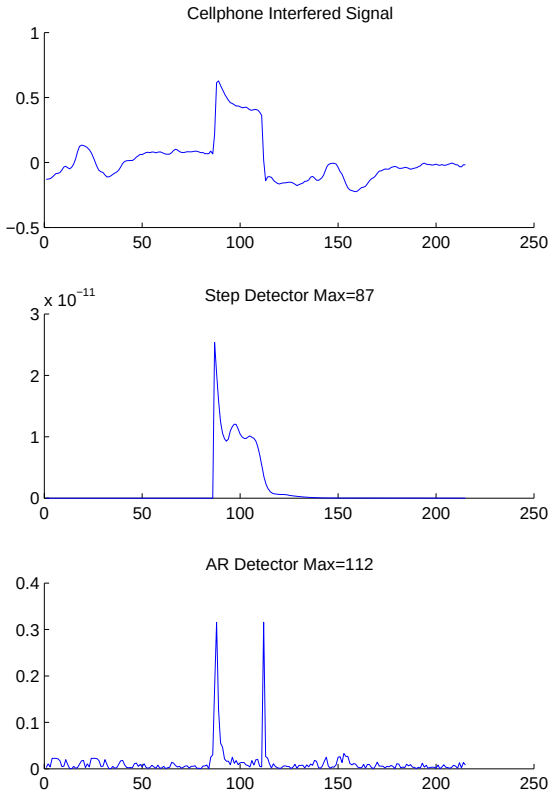

Figure 10: *Detection results of Bayesian step detector and AR detector.*

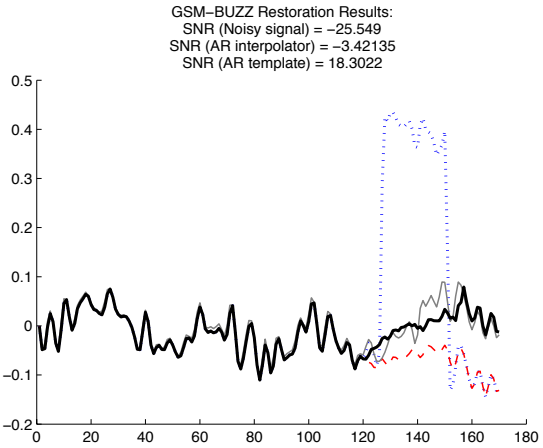

Figure 11: *Example of GSM buzz restoration of a corrupted vocal sequence (Pop):* $x(n)$ *(Dotted),* $s(n)$ *(Gray),* $s^0(n)$ *(Dashed),* $s^1(n)$ *(Black).*

7. REFERENCES

[1] B. Poole, "Reducing audio "buzz" in GSM cell phones," *EDN*, Feb. 2005, [Online] http://www.edn.com/article/CA498768.html.

[2] I. Claesson and A. Nilsson, "GSM TDMA frame rate internal active noise cancellation," *Inter. J. Acoust. and Vibration*, vol. 8, no. 3, pp. 159–166, 2003.

[3] J. J. Morrissey, M. Swicord, and Q. Balzano, "Characterization of electromagnetic interference of medical devices in the hospital due to cell phones," *Health Phys*, vol. 82, pp. 45–51, 2002.

[4] M. Skopec, "Hearing aid electromagnetic interference from digital wireless telephones," *IEEE Trans. Rehabil. Eng.*, vol. 6, no. 2, pp. 235–239, june 1998.

[5] M. Ross, "Telecoil and telephones the most commonly misunderstood "assistive listening device"," *Hearing Loss; The Journal of Self Help for Hard of Hearing People*, vol. 23, no. 1, pp. 16–19, Jan./Feb. 2002.

[6] G. B. B. Chaplin and R. A. Smith, "Method and apparatus for cancelling vibrations," U.S. Pat. 4490841, Dec. 1984.

[7] ——, "Hearing aid and method for operating a hearing aid to suppress electromagnetic disturbance signals," U. S. Pat. 20010762875, Aug. 1999.

[8] GSM Standard (GSM 05.01 version 7.0.0 Release 1998), "Digital cellular telecommunications system (phase 2+), Physical layer on the radio path," 1998.

[9] S. J. Godsill and P. J. W. Rayner, *Digital audio restoration – A Statistical model-based approach*. Springer-Verlag, 1998.

[10] J. J. K. O'Ruanaid and W. J. Fitzgerald, *Numerical Bayesian methods applied to signal processing*. Springer-Verlag, 1996.

[11] J. N. Bernardo and A. F. M. Smith, *Bayesian Theory*. Wiley, 1994.

[12] J. R. Bunch, "Stability of methods for solving Toeplitz systems of equations," *SIAM J. Sci. Stat. Comput.*, vol. 6, pp. 349–364, 1985.

[13] H. Lin and S. J. Godsill, "The multi-channel AR model for real-time audio restoration," in *IEEE Workshop on Audio and Acoustics*, Mohonk, NY State, Oct. 2005, pp. 1–4.